Energetic Particle Composition

Donald V. Reames

NASA Goddard Space Flight Center
Greenbelt, MD, USA

Abstract. Abundances of elements and isotopes have been essential for identifying and measuring the sources of the energetic ions and for studying the physical processes of acceleration and transport for each particle population in the heliosphere. Many of the sources are surprising, in a few cases the acceleration bias is extreme, but an understanding of the fundamental physics allows us to use energetic ions to determine abundances for the average solar corona, the high-speed solar wind, and the local interstellar medium.

INTRODUCTION

Energetic particles are accelerated by a variety of physical mechanisms at many sites throughout the heliosphere that may be listed as follows (see reviews by Lee (19) and Reames (36)):

Heliospheric Sources and Energetic Particles

1) Solar flares – ^{3}He/^{4}He and (Z>50)/O enhanced

2) CME-driven shock waves – large SEP events

3) Planetary magnetospheres
   a) Radiation belts – neutron albedo
   b) Io belt of S and O
   c) Trapped ACRs
   d) Ion conics

4) Planetary bow shocks
   – 'Upstream' events

5) Co-rotating interaction regions (CIRs)

6) Heliospheric termination shock
   – Anomalous Cosmic Rays (ACRs)
   – Interstellar pickup ions

7) Galactic Cosmic Rays (GCRs)

In recent years, we have learned to divide solar energetic particle (SEP) events into the small 'impulsive' events, accelerated in solar flares, and large, long-duration, 'gradual' events where acceleration occurs at shock waves driven out from the Sun by coronal mass ejections (CMEs) (9, 13, 14, 15, 17, 18, 36, 37). Resonant wave-particle interactions in flares can produce 1000-fold enhancements in ^{3}He/^{4}He and (Z>50)/O. On the other hand, abundances averaged over many large gradual SEP events allow the study of fractionation of the solar coronal material relative to the photosphere – the solar FIP (first ionization potential) effect. We are beginning to understand and model the dynamic physical processes of wave-particle interactions near shocks that explain abundance variations with time during one SEP event and from one event to another. We now see why averaging works. However, these abundances are complicated by shock re-acceleration of residual ions from impulsive flares, and by the exponential rollovers in the high-energy spectra, called spectral 'knees.'

Several magnetospheric populations have extremely interesting abundances. The main radiation belts of Earth, Jupiter, and Saturn consist almost entirely of the element H. This incredibly simple abundance pattern reveals the source of these belts as the decay of energetic neutrons that are produced by interactions of GCRs with the atmospheres, rings, and moons of these planets. Another interesting population, seen in the Jovian magnetosphere, has comparable abundances of S and O at several MeV/amu, without accompanying Ne, Mg, or Si. The S and O are accelerated from disassociated gasses such as SO_2 emitted from the volcanoes of the Jovian moon Io. Surely, this is the 'smoking gun' of abundances.

The anomalous cosmic rays (ACRs) are an example of an extreme FIP-based, ion-neutral separation of

a source population. Low-FIP ions are ionized in the local interstellar medium, but high-FIP ions, such as H, He, N, O, Ne and Ar, are mostly neutral. The neutrals easily cross magnetic fields to enter the heliosphere; if they are ionized by solar ultraviolet or by charge exchange with solar-wind protons, they are 'picked up' by the solar wind and carried out to the heliospheric termination shock where they are accelerated to produce ACRs. The distribution function of the interstellar pickup ions remains flat out to twice the solar wind speed where they greatly outnumber normal solar wind ions, providing preferential injection. The existence of the interstellar pickup ions was predicted by Fisk, Kozlovsky, and Ramaty (7) to explain ACRs well before these ions were actually observed in the solar wind, although the pickup of interstellar He had been suggested previously to explain He^+ in the solar wind (11). Abundances of the local interstellar medium can be determined from ACRs and pickup ions given suitable models of photo-ionization and charge exchange. Modeling is not required to determine isotopic ratios such as $^{22}Ne/^{20}Ne$ ~0.1 (20)

Corotating interaction regions are produced where high-speed solar wind streams overtake slower solar wind emitted earlier by the rotating Sun. From this interaction, a forward shock propagates out into the slow wind and a reverse shock propagates sunward into the high-speed stream. Particles are accelerated at both shocks but are more intense at the reverse shock. Particle intensities at the shocks increase with distance out to 5-10 AU. Energetic ions streaming sunward from the reverse shock, measured near Earth, appeared to represent the abundances of the high-speed wind (45). Later, however, these ions were thought to originate from singly ionized 'inner-source' pickup ions from solar wind that is absorbed, neutralized, and re-emitted at interstellar dust grains passing near the Sun (8). Ionization-state measurements of these energetic ions from CIRs, reported by Möbius *et al.* (30) at this workshop, indicate that the ions (with the exception of ~25% of He and ~8% of Ne) are multiply ionized and hence they are accelerated from the high-speed solar wind after all. We have come full circle.

Nearly all of the heliospheric sources are 'invisible,' in that ion acceleration produces no measurable photons, so we must derive the physics from the energetic particles themselves. This requires that we distinguish the influences of injection, acceleration, and transport. Improving observations and models of this rich variety of events and sources have begun to make this possible. Many of the properties of the energetic-particle populations have been discussed in previous review articles (19, 36) and will not be repeated here. This review will focus on those recent observations and new theories and models that have extended our understanding or revised our perspective of energetic particles and their underlying source abundances.

IMPULSIVE SOLAR FLARES

Energetic particles from impulsive solar flares are characterized by extreme abundance enhancements resulting from acceleration by resonant wave-particle interactions in the flare plasma (*e.g.* 36, 47, 48). All of the elements through Si are fully ionized, and Fe of charge ~20 is observed (22, 29), indicating flare-heated plasma at a temperature of ~10 MK.

Enhanced abundances similar to those seen in energetic particles are also deduced from the Doppler-broadened γ-ray lines emitted from the energetic ions in solar flares (23, 31). Narrow γ-ray lines emitted from the ambient flare plasma show normal coronal abundances with no enhancements. Thus, the enhancements arise during acceleration.

Recent observations on the Wind spacecraft have yielded abundances for the dominant element groups in the $34 \le Z \le 82$ region (39). These abundances, along with those for $Z \le 26$ (36, 39, 41), are shown in Figure 1 as enhancements relative to coronal abundances. Abundance enhancements at high Z have been confirmed by Mazur *et al.* (25) at this workshop.

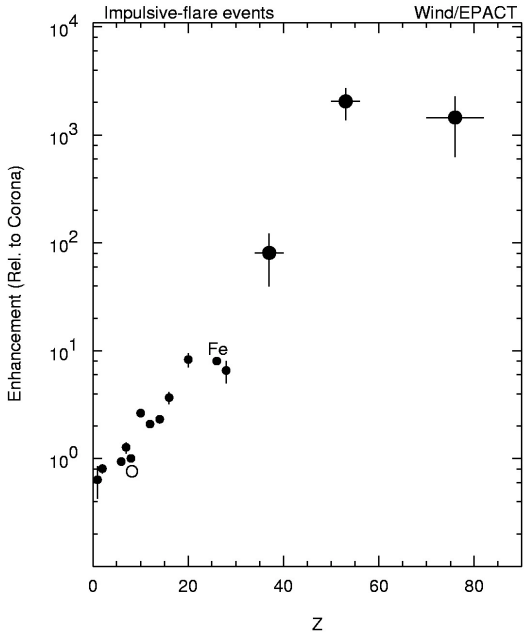

FIGURE 1. Abundance enhancements of heavy ions from impulsive solar flares.

Progressive enhancements of heavy ions may result from the physics of cascading waves (28) in which turbulent energy is generated at a large spatial scale and small wave number *k*, by magnetic reconnection above a flare. This energy Kolmogorov-cascades toward higher *k* and is first absorbed by ions with the lowest gyrofrequency and charge-to-mass ratio *Q/A*. Energy not absorbed by the heaviest ions continues to cascade toward lighter and lighter ions and is eventually absorbed by He or H.

Cascading waves may explain the abundance pattern in Figure 1, but, unfortunately, cannot explain the enhancements in ^{3}He/^{4}He. This enhancement is believed to result from electromagnetic ion cyclotron (EMIC) waves produced between the gyrofrequencies of H and ^{4}He by electrons streaming down the magnetic field lines (47, 48). ^{3}He is the only species whose gyrofrequency lies in this region so it can efficiently absorb these waves. A similar mechanism produces 'ion conics' in the Earth's auroral region where electrons, ions, and waves can all be observed *in situ*.

The necessity for two acceleration mechanisms, with unknown spatial and temporal relationships, makes it difficult to understand ion acceleration in flares. The necessity for acceleration before further ionization and the lack of correlations in the abundance variations complicate the picture (38, 41).

GRADUAL SEP EVENTS

In essentially all of the large SEP events particles are accelerated at CME-driven shock waves (9, 13, 14, 15, 18, 19, 36, 37). Peak particle intensities are correlated with CME speed and only 1-2% of CMEs drive shocks that are fast enough to accelerate ions (37). Shocks from the largest, fastest CMEs span more than half the heliosphere. These shocks expand across magnetic field lines accelerating energetic particles as they go.

Owing to the spiral pattern of the interplanetary magnetic field lines, which the ions follow, the particle time profiles depend in a systematic way upon the longitude of the observer relative to the source, as shown in Figure 2 (4, 36, 40). An observer on the east flank of the shock sees a source at a western longitude on the Sun. As a function of time, this observer's connection point swings from the intense nose of the shock, near the Sun, to the weaker flank when the shock arrives at 1 AU. An observer on the west flank of the shock may see maximum intensity only after crossing through the shock into the region where field lines connect to the shock nose from behind. Acceleration may also weaken, especially at high energies, as the shock moves outward, but the relentless eastward swing of the observers connection point to the shock is always a major factor.

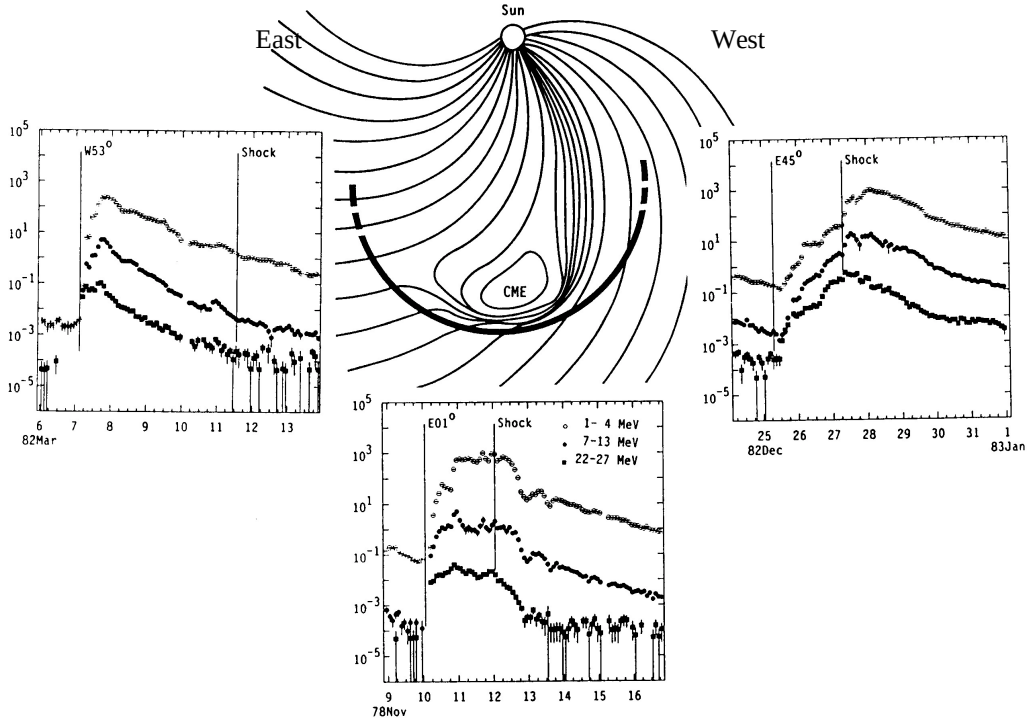

FIGURE 2. Intensity-time profiles for protons are shown for observers viewing a CME from three different longitudes.

A sufficiently fast CME near central meridian will produce an intensity peak at the time of shock passage (not seen in Figure 2), followed by a sharp decrease in intensity when the observer enters the CME or magnetic cloud, as is clearly seen in Figure 2. The reduced intensity inside the CME shows that little or no acceleration occurs at reconnection regions or other shock waves that might be *behind* the CME. Occasionally, however, new events at the Sun do fill this region behind the CME with energetic particles.

Average Abundances in Gradual Events

Historically, gradual SEP events have been used as a proxy for average coronal abundances. In his classic review, Meyer (26) realized that two different processes control SEP abundances when compared with photospheric abundances: 1) systematic event-to-event variations that depended upon *Q/A* of the ion (his 'mass bias') and 2) an overall dependence of the coronal source abundances on the first ionization potential (FIP) of the ions. Meyer also recognized impulsive ^{3}He-rich events as a separate population that he discussed in an appendix.

Breneman and Stone (2) significantly increased the number of elements measured and studied the *Q/A* dependence for 10 large SEP events observed on the Voyager spacecraft. They used the average *Q/A* values measured on ISEE-3 by Luhn *et al.* (22) and assumed that ionization states did not vary from event to event. They found a power-law dependence of enhancement *vs. Q/A* for ions with $Z \geq 6$ in several events, and they listed a complete set of average SEP abundances. If they had compared with modern photospheric abundances (10), they would have found no net *Q/A* dependence in their SEP averages.

Reames (35) determined SEP abundances averaged over 49 large events and examined variations. In Figure 3 these averaged SEP abundances are divided by the corresponding photospheric abundances (10) and plotted *vs.* FIP. The element H, which was neglected in early papers, has been included in this plot.

Evidence that averaging compensates for *Q/A*-dependent effects is seen by comparing Mg and Si with Fe in Figure 3. These elements have the same FIP but greatly different values of *Q/A*, yet they agree within statistical errors as seen in the Figure 3. The averaged SEP abundances for dominant elements have changed little in the last 15 years. However, abundances for the rarer elements have been improved and extended by Cohen *et al.* (5) at this workshop.

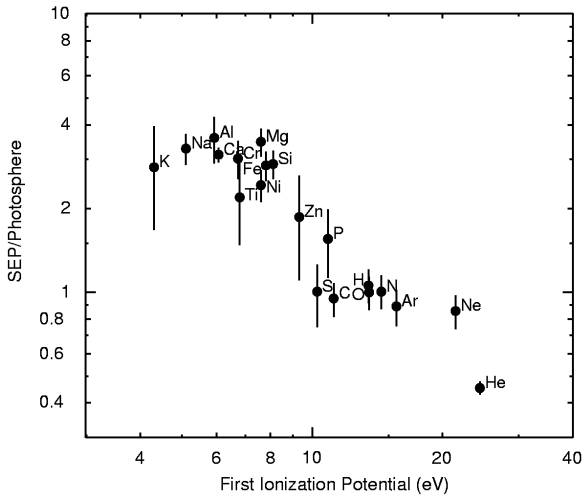

FIGURE 3. Averaged SEP coronal abundances relative to photospheric abundances are shown as a function of FIP.

Understanding SEP Abundance Variations

Unfortunately, the early treatment of SEP abundances and their variation from event to event was highly phenomenological. It left nagging questions. Why does averaging work so well? What actually causes the variations with *Q/A*. Why should a power-law organization exist and why does it break down? Why does H fit the *Q/A* phenomenology so poorly that it was completely ignored in early papers?

To answer these questions and to gain confidence in the relevance of SEP abundances as a proxy for coronal abundances, we must explore the physics of particle acceleration and transport. This necessity became even more compelling when new instruments showed systematic abundance variations with time during individual events, as shown in Figure 4 (36, 52). Note the different behavior of Fe/O in the two events and the uncorrelated variation in H/He.

Particles are accelerated at shocks because they gain an increment in velocity each time as they scatter back and forth across the velocity gradient of the shock (12, 17). At injection, the particles begin to scatter on ambient magnetic turbulence. As their velocity increases, those that begin to stream away from the shock generate or amplify resonant Alfvén waves of wave number, $k_{res}=B/\mu P$, where P is the particle's magnetic rigidity and μ the cosine of its pitch angle. Particles of the same rigidity that follow are scattered by the waves and increasingly trapped near the shock where they are further accelerated.

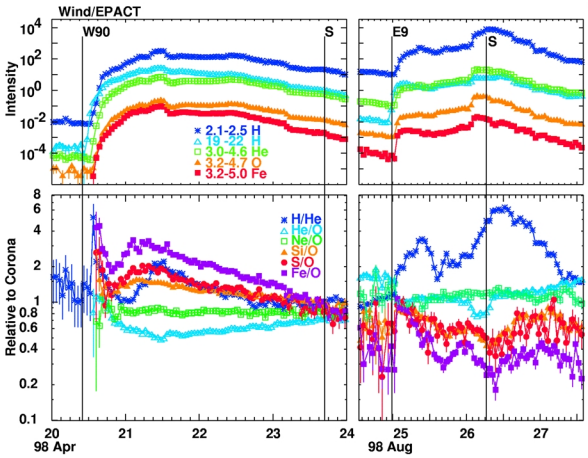

FIGURE 4. Selected intensities and relative abundances are shown *vs.* time for SEP events at two different longitudes.

At higher and higher energy, streaming particles grow new resonant waves. Eventually, at some high energy, the number of surviving particles becomes inadequate for wave growth to produce sufficient scattering, so these particles simply leak away from the shock. This leakage produces an exponential 'knee' in the particle spectrum that is otherwise a power-law in energy (3). We will discuss this knee in the next section.

Protons play a special role in wave generation at the shock. Since they are the most numerous species, they generate most of the waves, while the heavier ions act as test particles that probe the wave spectrum. SEP abundances are accumulated at the same velocity (*i.e.* energy/nucleon). However, ions with the same velocity will resonate with different regions of the wave spectrum because they have different values of *Q/A*, hence different rigidities. For wave spectra flatter than k^{-2}, for example, O will be scattered and trapped more efficiently than Fe of the same velocity, so that Fe/O is enhanced far away from the shock and suppressed nearer the shock.

Thus, Fe and O are merely redistributed in space along a magnetic flux tube by differential wave scattering. If we could integrate over space at a fixed time, we would obtain the coronal source abundances. However, since this is impractical, we can achieve a similar effect by averaging over SEP events at differing solar longitudes, since, as seen in Figure 2, events with western sources preferentially sample far ahead of the shock, and events with eastern sources preferentially sample near and behind the shock. *Abundance averaging over a large sample of events compensates for the spatial fractionation of elements by proton-generated Alfvén waves.* Of course, the abundances vary strongly with wave intensity even for events at a given longitude.

Detailed numerical calculations of Ng *et al.* (32, 33) follow the complete evolution of both particles and waves in space and time. These calculations can follow much of the complex behavior of abundances, as shown in Figure 5. The detailed time evolution depends upon the rate that the shock weakens; this is assumed to be linear in the simulation.

A critical feature of the wave-particle model has been the understanding it gives of the abundance of H, that was omitted in earlier studies. He/H and Fe/O are both ratios of high- to low-rigidity species at the same velocity. A power-law wave spectrum, like the Kolmogorov $k^{-5/3}$ spectrum, will produce power-law enhancements as a function of *Q/A*, so that He/H and Fe/O will behave similarly. Since the first particles to arrive propagate through a background Kolmogorov wave spectrum that is largely unmodified by wave growth, one might expect these ratios to begin at high values and decline with time. However, as shown in Figure 6, the ratios behave as expected in the 2000 April 4 event, but He/H behaves anomalously in the 1998 September 30 event (see also 43).

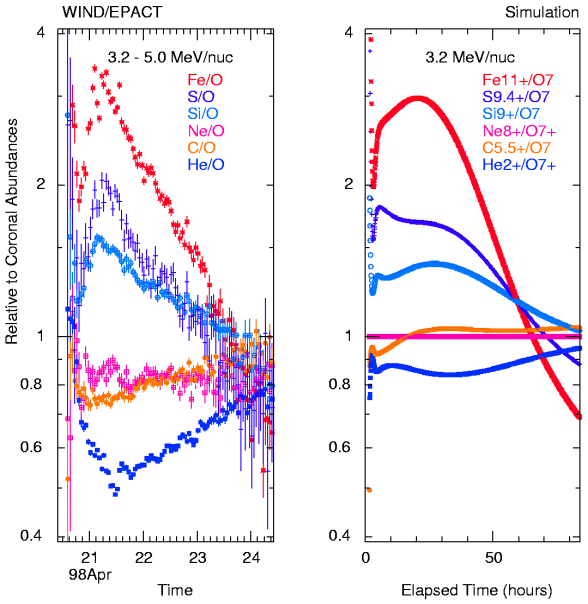

FIGURE 5. Comparison of observed and simulated abundance variations with time in the 1998 April 20 SEP event.

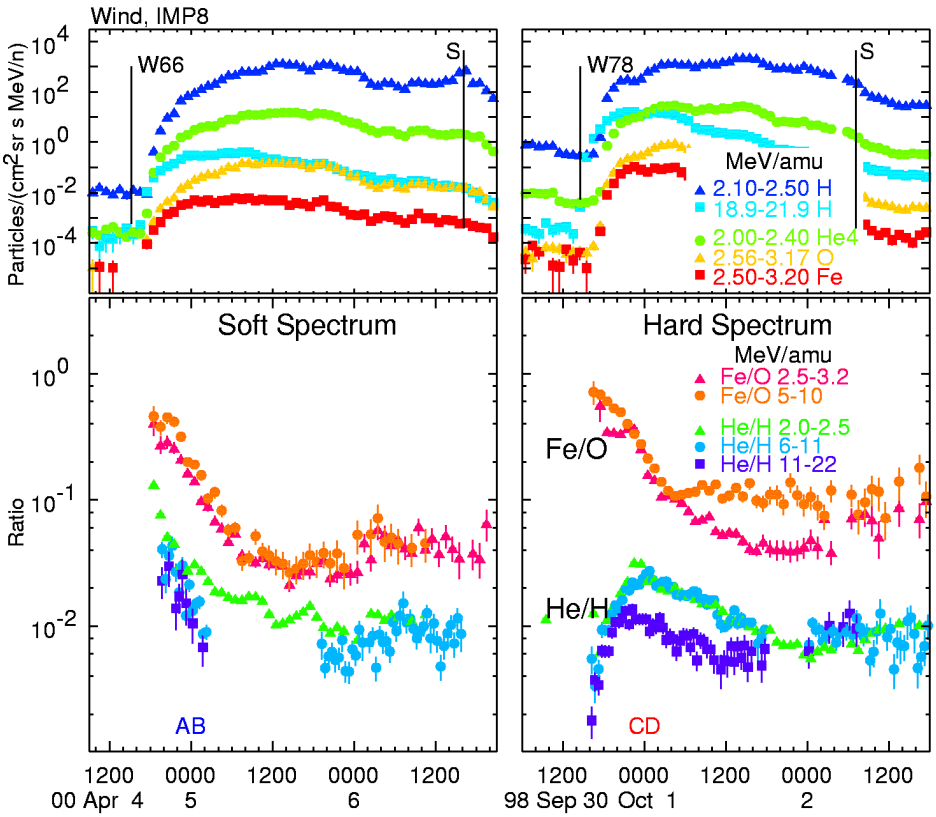

FIGURE 6. Time behavior of Fe/O and He/H are compared in the lower panels for two SEP events.

He/H ratios that initially rise with time can be explained because He of, say, 2 MeV/amu resonates with waves produced by protons of twice the velocity, *i.e.* at about 8 MeV. Thus, the He resonates with waves produced by protons that arrived much earlier. These protons have been producing waves much longer than the 2 MeV protons that just arrived. The spectral difference between these two events can be seen in Figure 7. The proton spectrum in the 1998 September 30 event is relatively hard, so there are enough high-energy protons to generate the waves necessary to preferentially scatter the He. The softer proton spectrum in the 2000 April 4 event does not produce enough waves. Proton intensities at 8 MeV and above differ by an order of magnitude for the two events. In these events, 8 MeV protons arrive 2-3 hrs before the onset of 2 MeV protons.

In addition to their effect on abundances, proton-generated waves control many aspects of energetic-particle behavior (37). They limit intensities early in events, flatten low-energy spectra (as seen in Figure 7), and rapidly reduce the streaming anisotropies in large SEP events. Even though the energy in proton-generated waves is limited to only a few percent of the energy in the protons themselves, the scattering that the waves produce greatly increases the acceleration efficiency of the shock, increasing attainable energies by factors of ~100 or more.

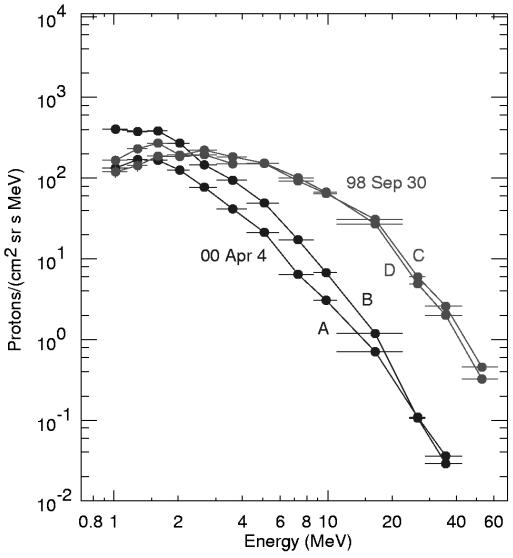

FIGURE 7. Proton energy spectra at times labeled A-D early in the two events shown in Figure 6.

Finally, it is important to realize that the transport of particles from SEP events may be complicated by

the presence of CMEs and shocks that exist in interplanetary space prior to the onset of a new event. The recent event on 2000 July 14 is shown in Figure 8 (44). Intensities of protons below 100 MeV suddenly increase at an intervening shock that arrives at Earth about 5 hours after the SEP event onset. Particle intensities remain relatively flat between this early shock and the source shock that arrives on July 15, suggesting that particles are partially trapped between the two shocks. This trapping most likely affects abundance ratios like Fe/O, which rises and remains elevated until the shock passage on July 15. This behavior contrasts with that of the 1998 August 24 event (Figure 4), which also comes from a source near central meridian, but has no intervening shock.

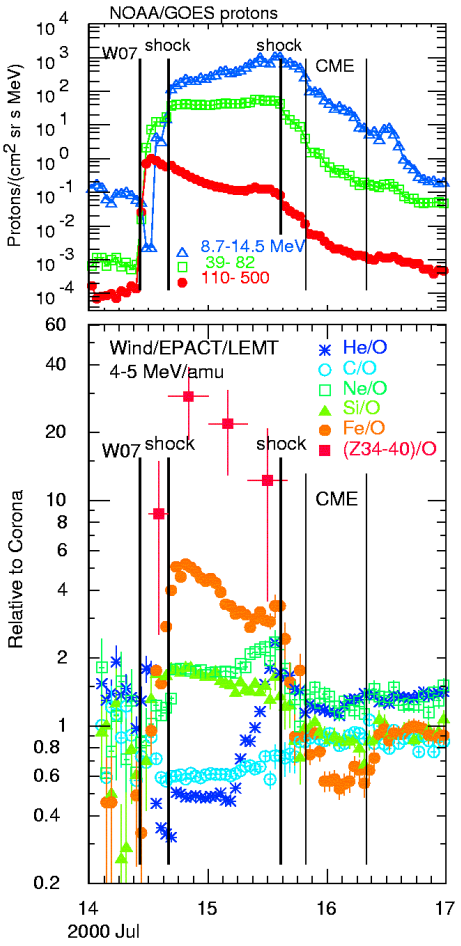

FIGURE 8. Proton intensities and relative abundances are shown *vs.* time for the 2000 July 14 event (44).

Spectral Knees

At sufficiently high energy, intensities of particles and resonant waves decrease, acceleration times increase, and particles leak away from the shock. The power-law spectrum of equilibrium shock acceleration is modified by the leakage (3) to a form such as $E^{-\gamma}\exp(-E/E_o)$ where we define the e-folding energy as the spectral 'knee' energy.

Tylka *et al.* (49) found that spectra in the 1998 April 20 event fit this form with $E_o = (Q/A)\,E_{oH}$, where E_{oH} is the knee energy for protons (see Figure 9). E_{oH} decreased slowly with time during the event from ~15 MeV to 10 MeV. Other events have a stronger or weaker dependence on Q/A and have larger variations of E_{oH} with time. Lovell *et al.* (21) derived the energy spectrum of the 1989 September 30 event using data from the ground-level neutron monitor network. For that event they found $E_{oH} \approx 1$ GeV. There are no instruments available to measure knee energies for ions above ~200 MeV/amu in SEP events.

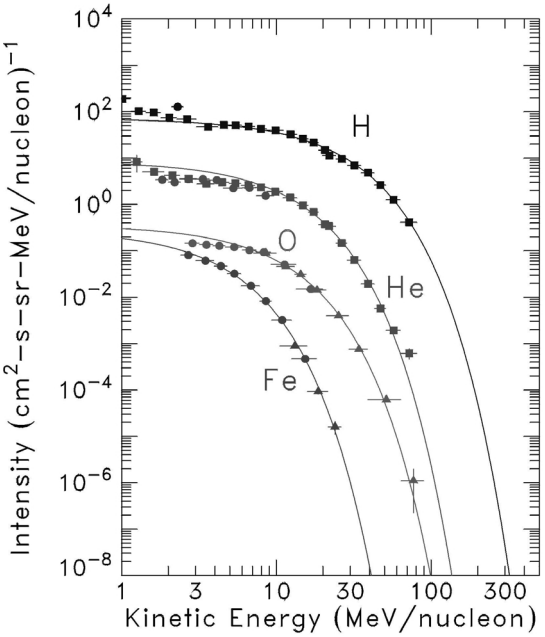

FIGURE 9. Ion spectra early in the 1998 April 20 event are fit to the form $E^{-\gamma}\exp(-E/E_o)$ by Tylka *et al.*(49) using data from IMP8, Wind, and ACE. E_o scales as Q/A in this event.

Spectral knees are a property of the acceleration, not a redistribution of particles in space. Therefore, averaging over events at energies above the knee will *not* recover coronal abundances.

The Seed Population

Shock waves accelerate ions from the high-energy tail of the thermal distribution. In the case of CME-driven shocks, ions from the corona and solar wind are

sampled as the 'seed population' for acceleration. Ionization states for the accelerated ions are typical of the solar wind or the 1-2 MK coronal plasma. Charge states of Fe from 10 to 15 are usually seen, even up to energies of 200-600 MeV/amu (50). In a few events the shock begins sufficiently low in the coronal plasma that energetic ions are further stripped, producing ionization states that increase with particle energy (42). The transport of Fe with charge 20 is different from that for Fe of charge 10. *Q/A*-dependent acceleration and transport affect the relative abundances of different ionization states of a single element just as they affect the relative abundances of elements.

Fast shocks will accelerate *any* ions that they encounter at suprathermal velocities, such as the pickup ions in the case of the heliospheric termination shock. Mason *et al.* (24) have suggested that an accumulation of suprathermal ^{3}He ions in the interplanetary plasma from many small impulsive flares during solar maximum could explain the small increases in ^{3}He/^{4}He~1% that they see in gradual SEP events. Enhancements of ^{3}He and heavy ions at interplanetary shocks were reported by Desai *et al.* (6) at this workshop. The accumulation of ^{3}He and Fe from small events during quiet periods at solar maximum has been known for many years (46).

However, the observational effects of shock acceleration of a suprathermal population of residual ions from impulsive flares are not limited to abundances of ^{3}He and Fe. To produce a final ratio of ^{3}He/^{4}He~1%, suppose we inject material with impulsive-flare abundances (36) and ^{3}He/^{4}He~1. Then ~10% of the resultant Fe will be from the impulsive population. Even if this does not noticeably alter Fe/O, it will contribute Fe ions of charges ~18-20 to the charge-state distribution, as is sometimes observed. In addition, adding an impulsive population to produce ^{3}He/^{4}He ~1% will also enhance (Z>50)/O by a factor of ~10. As an extreme example, an injection of impulsive suprathermal ions to contribute 10% of ^{4}He will contribute half of the final Fe, with Q_{Fe}~20, add 25% of the final Ne, and enhance (Z>50)/O by a factor of ~100. Enhancements in (34≤*Z*≤40)/O by a factor of ~30 are actually seen in the 2000 July 14 event, and are shown in Figure 8.

Abundances in impulsive SEP events are not well correlated among themselves, so it is difficult to establish correlated enhancements in ^{3}He/^{4}He and Fe/O. However, correlations between Fe/O, Ne/O, and Q_{Fe} have already been reported (29). Re-acceleration of suprathermal ions from prior impulsive flares can explain most of the events that are not 'pure' gradual events as judged by abundances or ionization states. However, injection of this flare population might alter the SEP average abundances somewhat.

A new chapter in the rapidly evolving story of 'remnant impulsive suprathermals' has just been written by Tylka *et al.* (51). Those authors assume a small 5% injection of impulsive suprathermals into the CME-driven shock, and they use observed charge distributions for the injected ions. Since the spectral knee energy varies as *Q/A* in many events, the high-*Q* suprathermals persist to higher energies than the accelerated lower-*Q* solar-wind ions. This simulation quantitatively fits the observed increase in Q_{Fe} at high energies in the 2000 July 14 and the well-measured 1992 November 1 events. This model also explains increases in Fe/O at high energy that, like the increase in Q_{Fe}, were not understood previously.

If re-acceleration of suprathermal ions from small impulsive SEP events is important, injection of suprathermal ions from prior gradual events must also be important. However, because the latter abundances and ionization states are similar to those of the solar wind, this process is difficult to establish. Nevertheless, the efficient injection of suprathermal ions may increase the maximum particle intensities and energies that can be attained at a shock. Kahler *et al.* (16) found that 'overachievers,' events with peak intensities above the correlation line of peak intensity *vs.* CME speed, were often those that followed immediately behind another large event.

Does the FIP-Level Vary?

For many years, spectroscopic observations have shown that the amplitude of the FIP effect varies by large factors throughout the solar atmosphere (*e.g.* 53). However, SEP events might be expected to average over large regions of the corona so they would smooth these variations.

To study event-to-event variations in the FIP level, we must overcome complex *Q/A* dependences. Reames (34) showed that that a ratio of neighboring elements, such as Mg/Ne, had little correlation with Fe/O, so that *Q/A* variations might be minimal. Figure 10 shows Mg/Ne for 43 events as a function of time over a solar cycle. For this sample, the weighted mean separation of the FIP levels is 4.06±0.03. The variance of a single event from this mean is 18%. Presumably these variations come from uncorrectable (nonlinear) dependence upon Q/A, complicated by time dependence in the abundances like those shown in Figures 4, 5, 6, and 8.

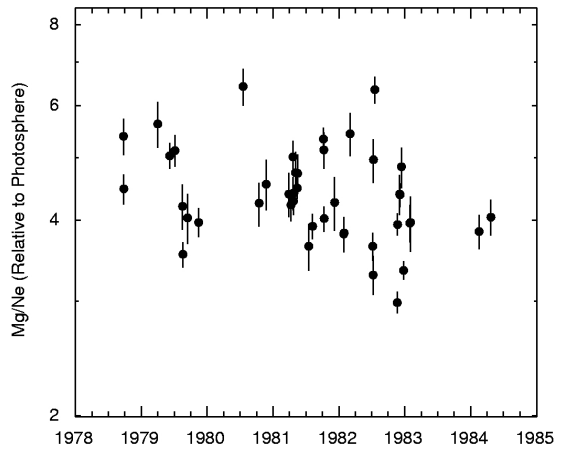

FIGURE 10. Mg/Ne is shown *vs.* time for 43 large SEP events (34).

More recently, Mewaldt *et al.* (27) fit the abundance enhancements to a power law in *Q/A*, treating the FIP level as an adjustable constant. They found somewhat larger variations. One wonders if part of the variation in the adjustable FIP level merely provided a partial compensation for the nonlinear departures from a power law in *Q/A* that are known to exist (see Figure 3.8 in reference 36). These authors also found a mean FIP amplitude of 4.0.

COROTATING INTERACTION REGIONS

As mentioned in the Introduction, ions accelerated from the high-speed solar wind at the reverse shock of CIRs were once believed to represent the abundances of the high-speed wind and the region above solar coronal holes (45). The abundances, averaged over 25 CIR events are shown, relative to photospheric abundances (10), as a function of FIP in Figure 11. While the statistics are somewhat poorer here than in SEP events, a smaller enhancement of low-FIP ions is seen in Figure 11 in comparison with Figure 3. It was known that interstellar He pickup ions could contribute to the energetic He from CIRs, but other pickup ions, such as O are rare in the inner heliosphere.

One of the historic problems with the abundances of energetic ions from CIRs is that the observed ratio of C/O= 0.89±0.05 is substantially larger than that of the SEP corona (0.465±0.013), photosphere (0.49± 0.10), or solar wind (0.71±0.07). Worse, the ratio seems to increase with the solar wind speed (36). No comparable variations are seen for C/O in SEP events although the range of corresponding shock speeds in SEP events is much greater than in reverse CIR shocks. However, differences between the solar wind and the photosphere and corona are also not understood.

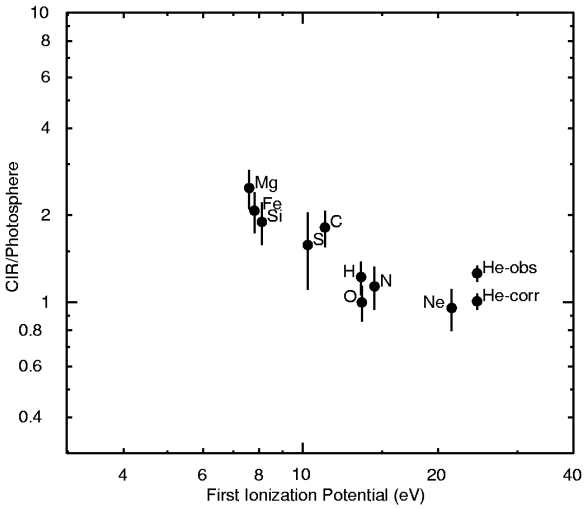

FIGURE 11. Average abundances of energetic ions from the reverse shock at CIRs, relative to the photosphere (10), are shown as a function of FIP. The element He is shown as observed and as corrected to remove interstellar pickup ions (see text).

The high value of C/O could not be explained by the presence of interstellar pickup ions, since C is suppressed in this population. A possible explanation advanced for the excess C was the 'inner source' of interstellar grains (8). Solar wind that is stopped by the grains and neutralized is subsequently 'recycled' and evaporated as neutrals that are photoionized and picked up by the solar wind. These singly charged ions C^+, O^+, and Ne^+ observed in the solar wind are attributed to the inner source (8). However, the distribution functions for these ions are well below those of the solar wind at all speeds. While the inner-source ions do have $C^+/O^+ \geq 1$, it is not clear why they would be preferentially accelerated.

Recent measurement of the ionization states of the energetic ions at 1 AU (30) show that most of the ions have charge states like those of the solar wind. The exceptions are that ~8% of Ne and ~25% of He are singly ionized, probably coming from the *interstellar* pickup-ion source. Thus, with these corrections, the abundances measured at 1 AU and shown in Figure 11 do indeed correspond to abundances of the fast solar wind. The correction for Ne is within errors, but the observed and corrected abundances for He are both shown in the figure. We have come full circle. However, the problem of explaining the high C/O has also returned.

SUMMARY

Energetic particle populations in the heliosphere come with a rich variety of abundances. They range from nearly pure H in radiation belts to flares with 1000-fold enhancements of heavy elements. The abundances reflect those of the underlying source plasma, as modified, in many cases, by fractionation processes that occur during injection, acceleration, and transport. Our challenge is to unravel these processes by distinguishing their dependence upon species, energy, and time.

Outside of regions of high magnetic fields such as planetary magnetospheres and solar flares, *all* of the sources seem to involve acceleration by collisionless shock waves. Gradual SEPs from CME-driven shocks, upstream particles from planetary bow shocks, CIRs, ACRs, and GCRs all allow us to probe the subtleties of shock acceleration with different source populations, shock parameters, and transport conditions. *All* of these sources show some degree of ion-neutral fractionation based upon FIP or a related variable. Gradual SEP events reflect abundances of the average corona and slow solar wind. CIRs and planetary bow shocks primarily reflect the fast solar wind that creates the highest shock speed. ACRs reflect the local interstellar medium as processed through the interstellar pickup ions, and GCRs reflect distant interstellar regions.

The self-consistent treatment of shock acceleration, based upon particle scattering by self-generated waves, was first applied to GCR acceleration (1), but has now been extended to other sources (12, 17). However, the time-equilibrium solutions that work well for slowly evolving shocks are ill suited to the unusually dynamic evolution of 'gradual' SEP events. With the aid of time-dependent models of abundance variations that have been developed recently, however, we are beginning to replace phenomenology with physical understanding.

For 16 years, the abundances averaged over many gradual SEP events at energies of a few MeV/amu, have served as a proxy for the average coronal abundance (26). We now understand this to be a natural consequence of using SEP events at different solar longitudes to sample the spatial redistribution of particles whose overall abundances are conserved to first order. Comparison of event-to-event spreads of Mg/Ne with those of Si/Mg or C/O, show that the FIP level varies less than 5-10% for events over a decade.

Abundance enhancements that exhibit a power-law dependence on *Q/A* (2) are produced when the spectra of the waves scattering the particles is a power-law flatter than k^{-2}, such as the $k^{-5/3}$ Kolmogorov spectrum. However, this behavior is usually seen only in small events or at extreme longitudes on the weak flanks of the CME-driven shock. In large events with strong wave growth, neither the wave spectra nor the abundance enhancements are power laws.

The erratic behavior in the abundance of H relative to other elements discouraged early workers from including H in SEP abundance tables. As the most abundant species, H dominates the production of particle-generates waves. Much of the behavior of He/H, for example, can be understood in terms of proton-generated waves. The element H can now be included with reasonable confidence.

Energy spectral knees, with their own species dependence, can distort the measure of coronal abundances, especially at high energy. Injection of a seed population of residual suprathermal ions from impulsive SEP events into the CME-driven shock can contribute enhancements in ^{3}He/^{4}He or Fe/O and elevated Q_{Fe} in gradual events. This explains the existence of 'mixed' or 'impure' gradual events, but it also suggests the need for a correction to SEP coronal abundances for some events.

SEP abundances from impulsive flares are acceleration dominated. They tell an interesting and complex story about resonant stochastic acceleration, but provide little information on coronal abundances. However, narrow γ-ray lines from flares do measure coronal abundances, while broad lines suggest the same enhancements seen in impulsive SEP events.

Energetic ions from the reverse shock in CIRs are a measure of abundances in high-speed solar wind streams that emerge from coronal holes. ACRs are an indirect measure of abundances in the local interstellar medium, although the origin of the rare low-FIP ions remains uncertain.

Energetic ions are a rich source of information about a variety of fundamental processes that take place in the heliosphere.

ACKNOWLEDGMENTS

I gratefully acknowledge the contribution made by Chee Ng, to this paper and to my personal education during the last few years, and I thank Allan Tylka for many helpful discussions. I also thank two unnamed referees for helpful comments.

REFERENCES

1. Bell, A. R.: 1978, *Mon. Not. Roy. Astron. Soc.*, **182**, 147.

2. Breneman, H. H., and Stone, E. C., *Astrophys. J. (Letters)* **299**, L57 (1985).

3. Ellison, D., and Ramaty, R., *Astrophys. J.* **298**, 400 (1995).

4. Cane, H. V., Reames, D. V., and von Rosenvinge, T. T., *J. Geophys. Res.* **93**, 9555 (1988).

5. Cohen, C. M. S. *et al*., this volume (2001).

6. Desai, M. I. *et al.*, this volume (2001)

7. Fisk, L.A., Kozlovsky, B., and Ramaty, R., *Astrophys. J. (Letters)* **190**, L35 (1974).

8. Gloeckler, G., Fisk, L. A., Zurbuchen, T. H., and Schwadron, N. A., in *Acceleration and Transport of Energetic Particles Observed in the Heliosphere*, eds. R. A. Mewaldt, J. R. Jokipii, M. A. Lee, E. Möbius, and T. Zurbuchen, AIP Conf, Proc. **528**, 221 (2000).

9. Gosling, J. T., *J. Geophys. Res*. **98**, 18949 (1993).

10. Grevesse, N., and Sauval, A. J., *Space Science Revs*. **85**, 161 (1998).

11. Holzer, T. E. and Axford, W. I., *J. Geophys. Res*. **76**, 6965 (1971)

12. Jones, F. C., and Ellison, D. E., *Space Sci. Revs*. **58**, 259 (1991).

13. Kahler, S. W., *Ann. Rev. Astron. Astrophys.* **30**, 113 (1992).

14. Kahler, S. W., *Astrophys. J*. **428**, 837 (1994).

15. Kahler, S. W., *et al.*, *J. Geophys. Res*. **89**, 9683 (1984).

16. Kahler, S. W., Burkepile, J. T., and Reames, D. V., *Proc. 26th ICRC* (Salt Lake City) **6**, 248 (1999).

17. Lee, M. A., *J. Geophys. Res*. **88**, 6109 (1983).

18. Lee, M. A., in *Coronal Mass Ejections*, eds. N. Crooker, J. A. Jocelyn, J. Feynman, Geophys. Monograph **99**, (AGU press) p. 227 (1997).

19. Lee, M. A., in *Acceleration and Transport of Energetic Particles Observed in the Heliosphere*, eds. R. A. Mewaldt, J. R. Jokipii, M. A. Lee, E. Möbius, and T. Zurbuchen, AIP Conf. Proc. **528**, 3 (2000).

20. Leske, R. A. in *26th Int. Cosmic Ray Conf.* (Salt Lake City), eds. B. L. Dingus, D. B. Kieda, and M. H. Salamon AIP Conf. Proc. **516**, 274 (1999).

21. Lovell, J. L., Duldig, M. L., Humble, J. E., *J. Geophys. Res*. **103**, 23,733 (1998).

22. Luhn, A., Klecker, B., Hovestadt, D., and Möbius, E., *Astrophys. J*. **317**, 951 (1987).

23. Mandzhavidze, N., Ramaty, R., and Kozlovsky, B., *Astrophys*. *J*. **518**, 918 (1999).

24. Mason, G. M., Mazur, J. E., and Dwyer, J. R., *Astrophys. J. (Letters)* **525**, L133 (1999).

25. Mazur, J.E., Mason, G.M., Dwyer, J. R., Gold, R. E and Krimigis, S. M., this volume (2001)

26. Meyer, J. P., *Astrophys. J. Suppl.* **57**, 151 (1985).

27. Mewaldt, R. A., Cohen, C. M. S., Leske, R. A., Christial, E. R., Cummings, A. C., Slocum, P.L., Stone, E. C., von Rosenvinge, T. T., and Wiedenbeck, M. E., in *Acceleration and Transport of Energetic Particles Observed in the Heliosphere*, eds. R. A. Mewaldt, J. R. Jokipii, M. A. Lee, E. Möbius, and T. Zurbuchen, AIP Conf, Proc. **528**, 123 (2000).

28. Miller, J. A., and Reames, D. V., in *High Energy Solar Physics*, eds. R. Ramaty, N. Mandzhavidze, X.-M. Hua, AIP Conf. Proc. **374**, 450 (1996).

29. Möbius, E., *et al.*, in *Acceleration and Transport of Energetic Particles Observed in the Heliosphere*, eds. R. A. Mewaldt, J. R. Jokipii, M. A. Lee, E. Möbius, and T. Zurbuchen, AIP Conf, Proc. **528**, 131 (2000).

30. Möbius, E., *et al*., this volume (2001).

31. Murphy, R J., Ramaty, R., Kozlovsky, B., and.Reames, D. V., *Astrophys. J*. **371**, 793 (1991).

32. Ng, C. K., Reames, D. V., and Tylka, A. J., *Geophys. Res. Lett*. **26**, 2145 (1999).

33. Ng, C. K., Reames, D. V., and Tylka, A. J., *Proc. 26th ICRC* (Salt Lake City) **6**, 151 (1999).

34. Reames, D. V., *Proc. First SOHO Workshop* (ESA SP-348), 315 (1992).

35. Reames, D. V., *Adv. Space Res*. **15** (7), 41 (1995).

36. Reames, D. V., *Space Science Revs*. **90**, 413 (1999).

37. Reames, D. V. in *26th Int. Cosmic Ray Conf.* (Salt Lake City), eds. B. L. Dingus, D. B. Kieda, and M. H. Salamon AIP Conf. Proc. 516, 289 (1999).

38. Reames, D. V., in *High Energy Solar Physics: Anticipating HESSI*, eds. R. Ramaty and N. Mandzhavidze, ASP Conf. Series 206, 102 (2000).

39. Reames, D. V., *Astrophys. J.* (*Letters*), **540**, L111 (2000).

40. Reames, D. V., Kahler, S. W., and Ng, C. K., *Astrophys. J.* **491**, 414 (1997).

41. Reames, D. V., Meyer, J. P., and von Rosenvinge, T. T., *Astrophys. J. Suppl.*, **90**, 649 (1994).

42. Reames, D. V., Ng, C. K., and Tylka, A. J., *Geophys. Res. Lett.*, **26**, 3585 (1999).

43. Reames, D. V., Ng, C. K., and Tylka, A. J., *Astrophys. J. (Letters)* **531**, L83 (2000).

44. Reames, D. V., Ng, C. K., and Tylka, A. J., *Astrophys. J. (Letters)* **548**, L233 (2001).

45. Reames, D. V., Richardson, I. G., and Barbier, L. M., *Astrophys. J. (Letters)*, 382, L43 (1991).

46. Richardson, I. G., Reames, D. V., Wenzel, K. P. and Rodriguez-Pacheco, J., *Astrophys. J. (Letters)*, 363, L9 (1990).

47. Roth, I., and Temerin, M., *Astrophys. J.* **477**, 940 (1997).

48. Temerin, M., and Roth, I., *Astrophys. J. (Letters)* **391**, L105 (1992).

49. Tylka, A. J., Boberg, P. R., McGuire, R. E., Ng, C. K., and Reames, D. V., in *Acceleration and Transport of Energetic Particles Observed in the Heliosphere*, eds. R.A. Mewaldt, J.R. Jokipii, M.A. Lee, E. Moebius, and T.H. Zurbuchen, AIP Conf. Proc. 528, p 147 (2000).

50. Tylka, A. J., Boberg, P. R., Adams, J. H., Jr., Beahm, L. P., Dietrich, W. F., and Kleis, T., *Astrophys. J.* (*Letters*) **444**, L109 (1995).

51. Tylka, A. J., Cohen, C. M. S., Deitrich, W. F., Maclennan, C. G., McGuire, R. E., Ng, C. K., and Reames, D. V., *Astrophys. J.* (*Letters*), in press (2001).

52. Tylka, A. J., Reames, D. V., and Ng, C. K., *Geophys. Res. Lett.* **26**, 145 (1999).

53. Widing, K. G., and Feldman, U., *Astrophys. J.* **344**, 1046 (1989).